Russian Chemical Reviews **67** (7) 563 – 571 (1998)
© 1998 Russian Academy of Sciences and Turpion Ltd

UDC 539.219.3:669.094.3 – 977:541.135.4

Catastrophic oxidation of metals

V V Belousov

Contents

I.	Introduction	563
II.	Fast stage of catastrophic oxidation of metals	564
III.	Super-fast stage of catastrophic oxidation of metals	569
IV.	Conclusion	570

Abstract. The review deals with the current state of the problem of catastrophic oxidation of metals ('hot corrosion') caused by formation of a liquid corrosion product in a multi-component system. The kinetics, thermodynamics, and mechanisms of the two stages of accelerated oxidation of metals, namely, fast and super-fast stages, are considered with the copper–bismuth oxide system as an example. It is shown that the fast stage is caused by the formation of a liquid-channel grain boundary structure in the corrosion product, while the super-fast stage is caused by the high rate of dissolution of the oxide layer. The results of studies of the interaction of liquid phase with two-dimensional defects (grain boundaries) in solids are generalised. A model of catastrophic oxidation of metals is proposed. The bibliography includes 104 references.

I. Introduction

The creation of high-temperature corrosion-resistant materials intended for prolonged exploitation under extremely drastic conditions is a current task of materials science. Such materials are used in nuclear and fuel-based power industries, in space technology, and in other branches of industry. In most cases, composite materials based on metals, such as metal-ceramics, sintered powder compositions of metals with oxides, nitrides, and borides, as well as amorphous alloys are employed. The practical solution of problems involved in the creation of corrosion-resistant materials depends largely on the development of theoretical concepts in the field of high-temperature oxidation of metals.

By now, it has been reliably established that the rate of high-temperature oxidation of metals leading to the formation of dense scale is controlled by diffusion processes. The rate of metal oxidation is determined by bulk diffusion of the reacting ions and electron transfer through the growing scale. These aspects are described by the Wagner model [1, 2] which makes it possible to find quantitative relationships between the rate of metal oxidation, the type and extent of oxide disordering, and the partial pressure of oxygen as a function of the type of conductivity of the scale (ionic or electronic).

V V Belousov Open Joint Stock Venture 'Research Institute of Steel' Dubninskaya ul. 81a, 127411 Moscow, Russian Federation.
Fax (7-095) 485 43 95. E-mail: nsteel@dol.ru

Received 21 March 1997
Uspekhi Khimii **67** (7) 631 – 640 (1998); translated by S S Veselyi

However, in certain cases the rate of metal oxidation exceeds that predicted by the Wagner model by several orders of magnitude. This phenomenon referred to as catastrophic oxidation of metals (COM) [3, 4] may be caused by the following.

1. The loss of isothermicity in the oxidation zone. The rate of metal oxidation increases continuously with temperature. This occurs if the liberated heat of the exothermic reaction cannot dissipate efficiently. Hence, the temperature of the metal surface increases, and the oxidation accelerates continuously. At a sufficient rate of oxygen supply, this process can result in inflammation of the metal. Inflammation of niobium, tantalum, titanium, and some other metals has been observed under extremal conditions. [5, 6]

2. The formation of volatile oxides. For example, tungsten, molybdenum, vanadium, rhenium, and osmium form volatile oxides but no protective oxide films. [7 – 10]

3. The formation of a small amount of a liquid phase in the oxidation product. This may be exemplified by oxidation of alloys the components of which form low-melting oxides; oxidation of metals in an atmosphere containing vapour of low-melting oxides; direct contact of metals and alloys with low-melting oxides. Even the appearance of a small amount of a liquid phase in the scale can lead to the COM. [11 – 27]

In the latter case, two stages of COM, namely, fast and super-fast ones, can take place. [28 – 30] The fast stage is caused by the formation of a liquid-channel grain-boundary structure (LGBS) in the oxidation product [31, 32] and occurs by an electrochemical mechanism. The super-fast stage is caused by the high rate of dissolution of the protective oxide layer and occurs by a fluxing mechanism.

The term 'COM' has been first introduced by Leslie and Fontana [3, 4] for an abrupt (by several orders of magnitude) increase in the rate of metal and alloy oxidation under isothermal conditions in a medium containing low-melting oxides (oxides of molybdenum, vanadium, lead, *etc.*). This phenomenon is also named 'hot corrosion'. [33 – 38] Strictly speaking, this definition of COM refers only to the third case discussed above. The other cases do not fit the definition completely. In the first case, metal oxidation occurs under non-isothermal conditions (a continuous increase in temperature in the reaction zone; the theory of this process has been suggested by Zel'dovich [5, 6]) and is related mainly to the physics of burning. In the second case, the oxidising medium does not contain a foreign low-melting oxide.

In the present work, only the third case is considered in detail with the copper – bismuth oxide system as an example.

To date, some progress has been achieved in the investigation of COM. However, many key questions remain debatable or unclear. For example, the mechanism of anomalously fast mass

transfer in solids involving the liquid phase and the mechanism of formation of a distributed structure (LGBS) are obscure; the interaction of a liquid phase with two-dimensional defects of a solid have been studied insufficiently.

In this review, the author attempted to discuss, from common viewpoints (thermodynamic, kinetic, structural), the mechanism of the COM caused by the formation of a liquid corrosion product in a multi-component system.

II. Fast stage of catastrophic oxidation of metals

1. Oxidation kinetics, structure and composition of the reaction products

Let us consider COM with the copper–bismuth system as an example, which most fully reflects the general features characteristic of other systems. It is known [26, 27] that copper coated with a thin film of bismuth (10–100 μm) undergoes catastrophic oxidation in air at 770 °C (Fig. 1). The rate of copper oxidation does not depend on the starting state of bismuth but depends on its quantity (Fig. 2). It has been found [28, 29] that the rate of copper oxidation increases with the thickness of the coating to reach a maximum at ~100 μm thickness (Fig. 3). The process of COM is determined by a parabolic time law, which indicates that the process is diffusion-controlled.

$$\left(\frac{\Delta m}{S}\right)^2 = kt \qquad (1)$$

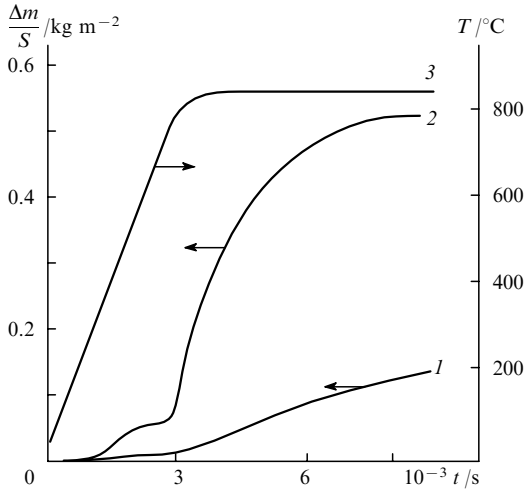


Figure 1. Kinetics of copper oxidation (*1*, *2*) and temperature change (*3*); *1*, without coating; *2*, coated with a 30 μm-thick bismuth film.

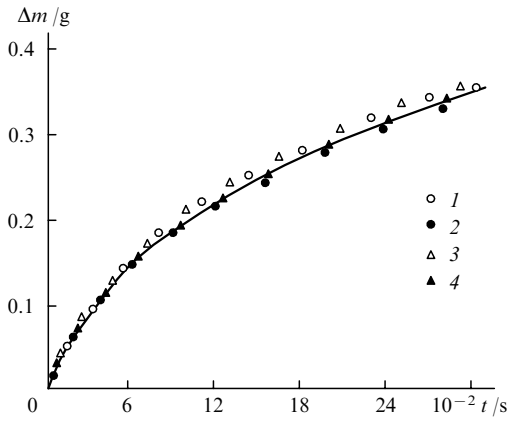


Figure 2. Kinetics of oxidation of copper with different coatings; (*1*), $Bi_2O_3 + Bi_2CuO_4$; (*2*), Bi; (*3*), Bi_2CuO_4; and (*4*), Bi_2O_3. In all cases, the amount of bismuth per unit area of copper is the same, $T = 800$ °C.

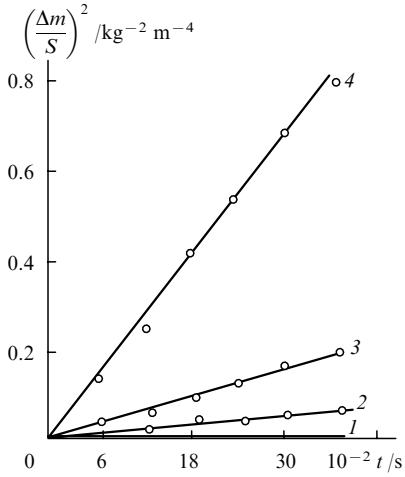


Figure 3. Kinetics of oxidation of copper coated with Bi_2O_3 films of different thickness at $T = 800$ °C. Film thickness × 10^5 /m: (*1*), 0; (*2*), 3; (*3*), 6; (*4*), 9; $10^5 k$ /kg² m⁻⁴ s⁻¹: (*1*), 0.012; (*2*), 1.6; (*3*), 4.9; and (*4*), 21.

Here Δm is the change in the mass of the specimen, S is the area of the surface that undergoes oxidation, k is the oxidation rate constant, and t is time. The k value depends on the coating thickness and exceeds the scale-formation constant on copper by a factor of over 1000. The temperature of 770 °C (threshold temperature for catastrophic oxidation of copper in the phase diagram of $CuO-Bi_2O_3$, see Refs 39–47) corresponds to the melting of the eutectics between Bi_2O_3 and Bi_2CuO_4. The COM process is associated with the formation of a liquid phase in the reaction products.

The scale on copper consists of two layers, [26–29] *viz*., the inner dark layer and outer light layer with a distinct interface (Fig. 4). The outer layer is formed of Bi_2CuO_4 with minor amounts of Bi_2O_3, Cu_2O, and CuO. The inner layer is built of CuO with minor Bi_2CuO_4, Bi_2O_3, and Cu_2O. The concentrations of the latter two compounds increase abruptly near the copper surface. The distribution of elements across the scale is in quantitative and qualitative agreement with the phase distribution shown in Fig. 4.

The position of layers in the scale shows that copper is oxidised predominantly due to oxygen diffusion.

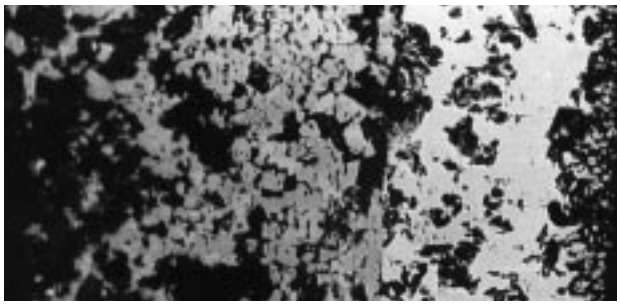


Figure 4. Microstructure of the scale on copper coated with a Bi_2O_3 film and oxidised in air at 800 °C; magnification is ×400.

2. Interaction of liquid phase with grain boundaries of the solid

Model experiments carried out in order to reveal the specific features of penetration of Bi_2O_3 and Bi_2CuO_4 into the bulk of CuO formed upon copper oxidation show that intense penetration of Bi_2O_3 or Bi_2CuO_4 (in liquid state) along CuO grain boundaries occurs at 770 °C (Fig. 5). The width of intergranular layers depends on the quantity of compound that has penetrated and can vary from fractions of a micron to several microns. The

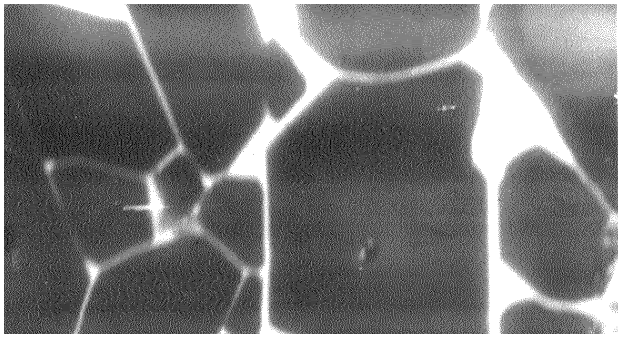


Figure 5. Microstructure of a CuO ceramics following thermal treatment in contact with Bi_2O_3 in air (cross-section).

penetration rate is high and reaches a few centimetres per minute (Fig. 6). The dependence of the penetration depth on time is linear. The activation energy of the process is 87±20 kJ mol^{-1}.

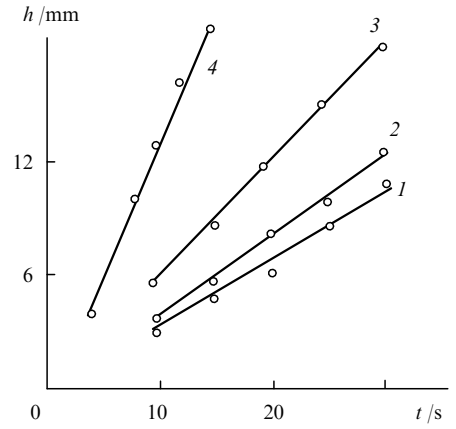


Figure 6. Dependence of the depth of penetration of the liquid phase (h) along CuO grain boundaries on time at different temperatures. T /°C: (*1*), 860; (*2*), 900; (*3*), 950; and (*4*), 1050.

The linear time dependence of the depth of penetration of the liquid phase along grain boundaries and its high rate indicate that the process is not diffusion-controlled.

3. Phase formation

According to the phase diagram, only one compound, namely, Bi_2CuO_4, is formed in the $CuO-Bi_2O_3$ system.[39–47] The amount of this compound decreases upon heating above 730 °C (Fig. 7).[32]

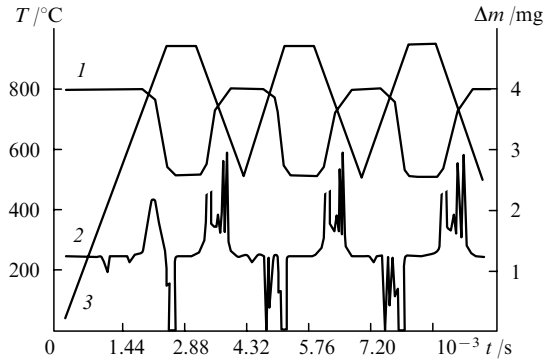


Figure 7. TGA (*1*), DTA (*2*), and T (*3*) curves for Bi_2CuO_4 exposed to cyclic heating and cooling in air.

The weight loss is accompanied by an exothermic effect on the DTA curve (*2*) and increases with temperature. The original weight is restored on cooling, but a small hysteresis appears on the TGA curve (*1*). The weight recovery is accompanied by additional exothermic effects corresponding to the reverse polymorphic transformation of Bi_2O_3, $\delta \rightarrow \gamma \rightarrow \beta \rightarrow \alpha$.[48–58] The weight loss is caused by partial dissociation of bismuth cuprate according to the reaction

$$2Bi_2CuO_4 \rightleftharpoons 2Bi_2O_3 + Cu_2O + 0.5O_2 \uparrow \quad (2)$$

The decomposition of polycrystalline Bi_2CuO_4 occurs both from the outer and inner surfaces (grain boundaries). A liquid phase is formed at grain boundaries (Fig. 8). The figurative point of the system in the phase diagram of $Bi_2O_3-Cu_2O$ (Fig. 9) with composition $2Bi_2O_3 + Cu_2O$ and a temperature of 730 °C is above the liquidus line, which corresponds to the liquid state. The volume fraction of the liquid phase increases with temperature. Hence, the equilibrium at the ternary diagram of Bi–Cu–O is shifted from the Bi_2O_3-CuO cross-section to the $Bi_2O_3-Cu_2O$ cross-section. The liquid phase forms a connected network of channels along Bi_2CuO_4 grain boundaries (see Fig. 8), thus forming an LGBS.[31,32] This implies that the thermodynamic condition of wetting, $\sigma_{gb} > 2\sigma_{sl}$ (where σ_{gb} is the surface tension of grain boundaries and σ_{sl} is the surface tension of the crystal–melt interface) is fulfilled. The exothermic effect at the DTA curve (first cycle, see Fig. 7) is probably related to wetting of grain boundaries with the liquid.

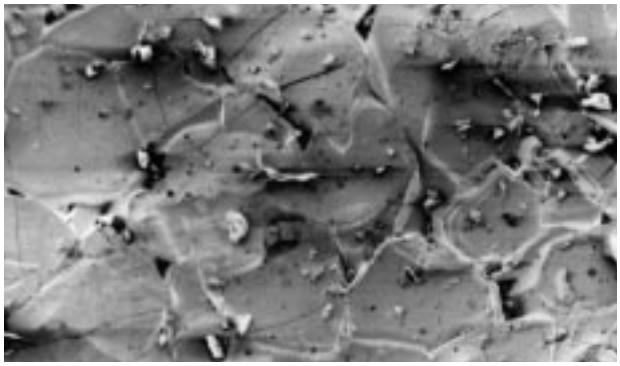


Figure 8. Microstructure of Bi_2CuO_4, quenching from 820 °C (fractured surface).

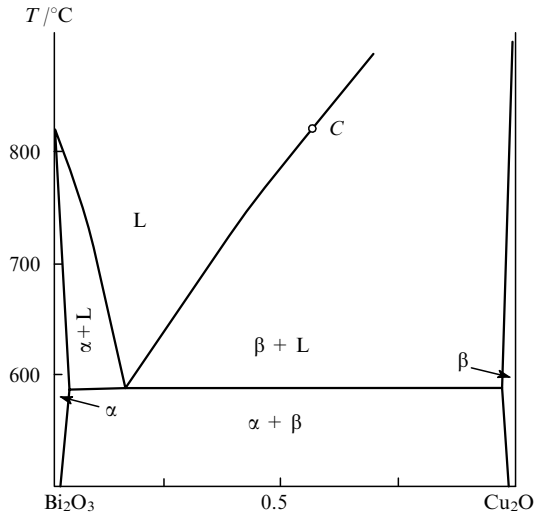


Figure 9. Cross-section of the phase diagram of Bi_2O_3-CuO, $p_{O_2} = 10^{-2}$ Pa. Point C corresponds to 60 mol.% of Cu_2O and 40 mol.% of Bi_2O_3, $T = 816$ °C.

4. Liquid-channel grain-boundary structures

Experimental results[26–29,31,32] provide a reason to believe that the liquid phase plays an important role in the COM. This phase interacts with two-dimensional defects (grain boundaries) to form an LGBS, which affects considerably the mass transfer in the solid.

In some instances, the contact of solids with liquids results in the formation of grooves where grains outcrop at the outer surface;[59–85] these grooves are characterised by a definite dihedral angle θ (Fig. 10). The value of θ is related to the surface tensions at the grain boundary and at the crystal–melt interface by a mechanical equilibrium at the groove apex:

$$\sigma_{gb} = 2\sigma_{sl}\cos\frac{\theta}{2}. \tag{3}$$

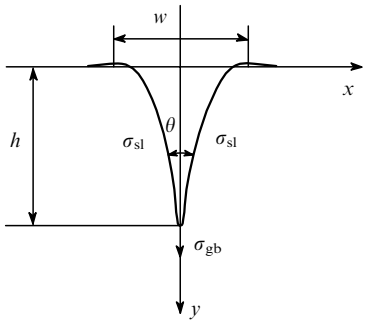


Figure 10. Profile of a grain boundary groove of liquid-phase etching.

A theoretical description of changes in topography of grain-boundary grooves and various transfer mechanisms is given by Mullins.[60,61] Let us briefly consider the Mullins theory of the development of a grain-boundary groove with a thermally etched groove as an example. Let a flat grain boundary outcrop at a flat surface (Fig. 10). The problem is to determine the surface profile at time t. The dependence of the chemical potential of an atom at a curved surface on the surface curvature is described by the Gibbs–Thomson equation

$$\mu_{i(L)} = \mu_{i(\infty)} + \Omega_i \sigma L, \tag{4}$$

where $\mu_{i(L)}$ and $\mu_{i(\infty)}$ are the chemical potentials of the i-th component at a surface of curvature L and at a flat surface, respectively, Ω_i is the partial volume of the i-th component, and σ is the surface tension. Hence, the chemical potential of an atom is determined by the surface curvature at this point

$$L = y'' \left[1 + (y')^2\right]^{-3/2}. \tag{5}$$

The value

$$\Delta\mu = \mu_{i(L)} - \mu_{i(\infty)} \tag{6}$$

reaches a maximum at $x = 0$ and decreases at $x > 0$ and $x < 0$. At the same time, $\nabla\mu$ is not equal to zero, causing a flux of atoms from the region with a higher potential (groove tip and banks) to that with a smaller potential (plateau), hence the groove should deepen and widen.

The dependence of the groove dimensions on time (t) is determined by the mechanism of the atom transfer. For example, for surface diffusion the groove width (w) and depth (h) are proportional to $t^{1/4}$:

$$w = 4.6(At)^{1/4}, \qquad h = 0.97(At)^{1/4}\operatorname{ctg}\frac{\theta}{2}, \qquad A = \frac{D_s\sigma\Omega^2 n_s}{kT}, \tag{7}$$

where D_s is the surface diffusion coefficient, n_s is the atom surface density, k is the Boltzmann constant, and T is temperature.

For bulk diffusion

$$w = 5(Bt)^{1/3}, \qquad h = (Bt)^{1/3}\operatorname{ctg}\frac{\theta}{2}, \qquad B = \frac{D\sigma\Omega^2\rho}{kT}, \tag{8}$$

where D is the bulk diffusion coefficient and ρ is the bulk density.

Quite a different physical picture appears if a fast diffusion pathway, such as liquid-phase diffusion, is possible. An analysis of the role of this process requires that the cases of saturated and unsaturated solutions are distinguished. The growth of a groove in a saturated solution occurs under the action of capillary forces. This process can be described using the Mullins theory, *i.e.* by the bulk diffusion of atoms through the liquid phase. This approach has been used repeatedly (see *e.g.*, Refs 76–78) to find that the groove width and depth change proportionally to $t^{1/3}$. Calculations agree satisfactorily with experimental data,[76] which shows that the maximum growth rate of the groove in this mode is as high as $\sim$0.5 mm h^{-1}. This value is considerably lower than that in the case of COM, where the liquid phase interacts with the grain boundaries of a solid (see Fig. 6).

Groove growth in unsaturated solution occurs under concentration gradient. Two extreme cases are possible. First, the process can occur in a kinetic mode ($h \sim t$, $w \sim t$), where the groove growth rate is controlled by dissolution, and diffusion transfer in the liquid phase occurs fast. Second, the process can occur in a diffusion mode ($h \sim t^{1/2}$, $w \sim t^{1/2}$), where the groove growth rate is controlled by diffusion through the liquid phase, and dissolution occurs rapidly. Calculations and experimental data[75] show that the maximum groove growth rate in the diffusion mode can be as high as several millimetres per hour, which is also much slower than in the case of COM.

The possibility of attainment of high rates of the groove deepening in the kinetic mode was considered by Fradkov.[81] It was shown that in narrow grooves the groove tip moves much faster than the banks, resembling the movement of scissors. The groove deepening rate (υ) is related to the rate of dissolution of a flat solid surface (υ_0)[81]

$$\upsilon = \frac{\upsilon_0}{\sin(\theta/2)}. \tag{9}$$

However, an estimate of v using this formula showed that it is physically unreal to reach rates of several centimetres per minute. Such a rate can only be obtained at $\theta \simeq 0.2'$. Hence the Fradkov model is not applicable, as also noted by the author. The situation changes if υ_0 increases. For example, this can occur if the groove deepening rate is controlled by the kinetics of channel opening at the tip rather than by that of the banks' expansion. It has been established experimentally that in the case of COM, where a liquid phase interacts with grain boundaries of a solid, the rate of the channel opening at the tip is controlled by the chemical reaction

$$CuO + Bi_2O_3 = Bi_2CuO_4. \tag{10}$$

It was noted above that Bi_2CuO_4 is thermally unstable and undergoes partial dissociation according to reaction (2). At grain boundaries, reaction (10) occurs, which [according to Eqn (2)] does not require any diffusion-controlled supply of the reagent, Bi_2O_3, or diffusion-controlled withdrawal of the product, Bi_2CuO_4. The oxygen evolved at the groove tip favours convective mixing (as the width of liquid channels exceeds considerably the free path of molecules).

Thus, fast penetration of a liquid along the CuO grain boundaries occurs due to acceleration of a chemical reaction at the grain boundaries rather than in the bulk. The most significant factors that favour the development of this process are the following: the chemical potential of atoms at the grain boundaries is higher than in the bulk; a chemical reaction occurs which does not require a diffusion-controlled supply of reagents (or diffusion-controlled withdrawal of products); a liquid, thermally unstable

product is formed; reaction is accompanied by gas evolution; a local temperature gradient appears due to a local chemical reaction; and the liquid is supplied to the channel by capillary forces.

The development of liquid channels occurs in the kinetic mode (see Fig. 6), hence equation (9) is still valid. However, v_0 acquires the meaning of the chemical reaction rate on a solid flat surface. Estimates show that the kinetic mode of the liquid channel growth controlled by a chemical reaction can result in narrow deep channels with a dihedral angle at the tip $0 < \theta < \pi$ at $\upsilon \sim 1$ cm min^{-1} and with υ_0 values $0.001-1$ cm min^{-1}, which are characteristic of topochemical reactions.[86,87] The activation energy of the process, 87 kJ mol^{-1}, is also typical of topochemical reactions.[86]

As a result of fast liquid penetration along the CuO grain boundaries, a continuous network of intergranular liquid channels is formed, eventually resulting in the LGBS formation.

Liquid-channel grain boundary structure can also be formed in different ways, *e.g.*, by topochemical decomposition of thermally unstable Bi_2CuO_4. In both cases, the LGBS formation manifests itself as a sharp increase in electric conductivity caused by the onset of high ionic conductivity due to the oxygen ions.[31,32] It has been shown[28,29] that an LGBS based on CuO (see Fig. 5) readily conducts the oxygen ions. The ionic conductivity reaches $\sim 1\ \Omega^{-1}$ cm^{-1} at 780 °C. The magnitude of conductivity is characteristic of superionic conductors.[88–92]

Judging by phase composition and structure, LGBS should be attributed to heterogeneous structures. The question about the passage of electric current through heterogeneous structures has been first raised by Maxwell.[93] In particular, he considered the conditions of the passage of current through a two-phase system, which is a continuous medium with randomly distributed spherical inclusions. Odelevskii[94] pointed out that heterogeneous structures can be organised in two ways. A feature of distributed matrix structures is that one of the two or several constituent phases always forms a bound matrix, however small volume the phase occupies. The phases constituting a statistically distributed structure do not form a bound matrix. Therefore, we shall treat LGBS as distributed matrix structures the matrix of which consists of liquid channels with a thickness from fractions of a micron to several microns localised at the grain boundaries.

In some cases, the ionic conductivity increases at a certain ratio of phases that form a distributed phase.[95–100] For example, the ionic conductivity can increase due to boundary phenomena on hetero-junctions.[98,99] This is caused by disordering of crystal lattices in boundary regions and an increase in the concentration of mobile carriers. This effect is only characteristic of ionic conductors whose conductivity originates from the Frenkel or Shottky defects. Analogous effects are also possible if segregation of an admixture on phase boundaries produces surface transition phases of a different chemical composition with enhanced conductivity.[100]

Unlike the distributed structures mentioned above, LGBS incorporates continuous liquid channels along the grain boundaries. These channels can serve as diffusion paths for ions, since the activation energy of diffusion in a liquid is much lower than that in a solid. Figure 11 shows the dependence of the effective diffusion coefficient (D_{ef}) in LGBS on the volume fraction of phases calculated according to Maxwell and Hart.[93,101] The diffusion coefficient in the solid phase was assumed to be $\sim 10^{-9}$ cm^2 s^{-1}. For example, D_{ef} is $\sim 10^{-6}$ cm^2 s^{-1} if the volume fraction of the liquid phase is 10%. Such a high diffusion permeability of LGBS is due to the presence of a highly conductive liquid matrix.

Thus, the high ionic conductivity of LGBS is caused by the formation of a distributed matrix structure rather than by structural disordering as is the case in superionic conductors.

5. Mechanism of the fast stage in the catastrophic oxidation of metals

The LGBS model makes it possible to explain the high COM rates. Before discussing the mechanism of copper catastrophic oxidation, let us accept several key assumptions.

1. A liquid layer is formed on the surface of copper due to thermal dissociation (or melting) of Bi_2CuO_4. Let us assume that reaction (2) involves at least two stages:

$$Bi_2CuO_4 \rightleftharpoons Bi_2O_3 + CuO\,, \tag{11}$$

$$CuO \rightleftharpoons 0.5Cu_2O + 0.25O_2\,. \tag{12}$$

Each of these steps has its own equilibrium constant. Since ionic bonds predominate in all of the above oxides, it may be assumed that further dissociation into ions occurs in the melt. As an example, let us express reaction (12) in the ionic form

$$CuO \rightleftharpoons (1-\alpha)Cu^{2+} + \alpha Cu^{+} + (1-\alpha/2)O^{2-} + (\alpha/4)O_2\,, \tag{13}$$

where α characterises the degree of CuO dissociation according to reaction (12). Reaction (13), which describes an equilibrium between ions in solution, was written assuming total dissociation of CuO. In reality, the degree of dissociation is much less than unity, therefore we shall consider the liquid layer as a dilute solution.

2. As a result of interaction of grain boundaries with the liquid phase, an LGBS is formed as a product of copper oxidation.

3. Copper is oxidised with oxygen dissolved in the liquid layer. The oxygen concentration is replenished continuously by the atmospheric oxygen.

4. The diffusion of oxygen ions through the liquid layer and liquid intergranular channels (Fig. 12) is the rate-determining step of the process.

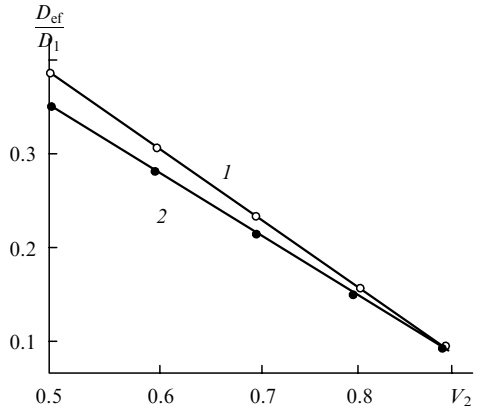


Figure 11. Effective diffusion coefficient of LGBS calculated according to Hart (*1*) and Maxwell (*2*); D_1 is the diffusion coefficient in the liquid phase ($\sim 10^{-5}$ cm^2 s^{-1}), V_2 is the volume fraction of the solid phase.

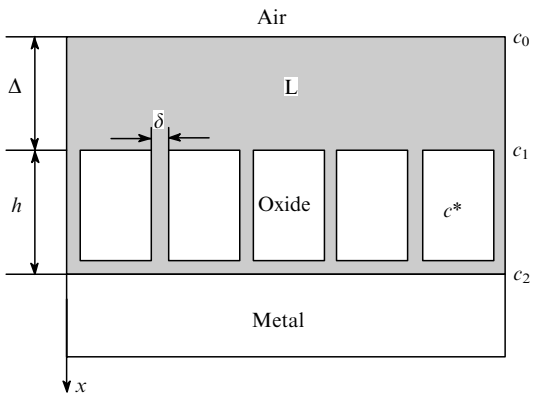


Figure 12. Topography of penetration of the liquid phase along the grain boundaries and interphase boundaries and a LGBS fragment in the catastrophic oxidation of copper.

5. The steady state is established locally all over the scale (where the scale is understood as the oxidation product + liquid layer).

6. The scale thickness is large in comparison with distances over which the effect of the bulk charge is felt (double electrical layer).

7. The solubility of oxygen in the metal can be neglected.

Let us consider the mechanism of diffusion growth of the oxide (see Fig. 12). Let us assume the thickness of copper oxide that formed to be h at time t and its growth to occur due to the oxygen supplied to the surface through liquid intergranular channels. If the concentration of oxygen in the growing oxide is designated as c^*, the mass balance equation is represented as follows

$$c^* \frac{\mathrm{d}h}{\mathrm{d}t} = J\,, \tag{14}$$

where J is the density of oxygen ion flux

$$J = -D\frac{\mathrm{d}c}{\mathrm{d}x}, \tag{15}$$

where D is the diffusion coefficient of oxygen ions and c is the concentration of the oxygen ions;

$$D = \frac{RT}{4F^2 c}, \tag{16}$$

where $\varkappa$ is the partial specific electric conductivity of oxygen ions and F is the Faraday constant.

Let us consider two variants of the COM model. In the first one, the liquid layer is a film of thickness $\Delta = 10-100$ μm, $\Delta \leqslant \Delta_{cr}$, and $\Delta \leqslant h$ ($\Delta_{cr} \simeq 100$ μm corresponds to the experimentally obtained film thickness at which the maximum rate of copper oxidation is observed).[28,29] It is assumed in this case that the material in the film is mixed and the concentration gradient of oxygen across the film thickness is absent. The oxygen concentration in the film is determined by dissociation equilibrium. However, a concentration gradient of oxygen exists in a liquid channel. The diffusion of oxygen occurs under permanent boundary conditions (stationary problem):

$$c\,(x = 0,\, t) = c_0\,,\; c\,(x = \Delta,\, t) = c_1\,,\; c\,(x = \Delta + h,\, t) = c_2. \tag{17}$$

Assuming a linear distribution of oxygen concentration in the channel, one obtains

$$\nabla c = \frac{c_1 - c_2}{h}. \tag{18}$$

The oxygen concentration c_2 is very small, so one may consider $c_2 = 0$ and (taking into account the mixing in a liquid film) $c_1 = c_0$. Thus,

$$\nabla c = \frac{c_0}{h}. \tag{19}$$

Substitution of equation (19) into (15) gives

$$J = -D\frac{c_0}{h}. \tag{20}$$

The equation of mass balance (14) for thin films, taking account of (20), takes the form

$$c^* l \frac{\mathrm{d}h}{\mathrm{d}t} = \delta D \frac{c_0}{h}, \tag{21}$$

(l is the mean grain size of copper oxide and δ is the width of a liquid channel in LGBS) or

$$c^* \frac{\mathrm{d}h}{\mathrm{d}t} = D_{ef}\frac{c_0}{h}, \tag{22}$$

where

$$D_{ef} = D\frac{\delta}{l}. \tag{23}$$

Separation of the variables in equation (22) and integration gives a parabolic law of copper oxidation

$$h^2 = kt\,. \tag{24}$$

Here k is the rate constant for copper oxidation

$$k = 2D_{ef}\frac{c_0}{c^*}. \tag{25}$$

The diffusion of oxygen anions along the liquid channel to the growing oxide surface is accompanied by a less intense counter-diffusion of copper cations into the film, which increases their concentration in the film. According to equation (13), this shifts the equilibrium to the left. As a result, the concentration of oxygen anions c_0, and hence k, decrease. If this phenomenon is named 'solution poisoning', it is obvious that the thinner the film the more pronounced this effect, and *vice versa*. Therefore, the dependence of k on the film thickness (for thin films, $\leqslant 100$ μm) can be explained by solution poisoning. This effect is insignificant and can be neglected for thick films.

Estimates show that if the degree of CuO dissociation according to reaction (12) equals unity and, accordingly, the degree of Bi_2CuO_4 dissociation according to reaction (11) is 0.25 (see Ref 59), and the degree of dissociation of Bi_2O_3 and Cu_2O into ions is about the same, the concentration of the oxygen anions in the liquid film is $c_0 \approx 0.03$ (in atomic fractions). The rate constant for copper oxidation under a thin layer of Bi_2CuO_4 is calculated according to the formula

$$k_{theor} = 2D_{ef}\frac{c_0}{c^*}\rho^2, \tag{26}$$

where ρ is the CuO density. At $c^* = 0.5$, $D_{ef} \approx 10^{-10}$ m^2 s^{-1}, and $\rho_{CuO} = 6.45 \times 10^3$ kg m^{-3}, we have $k_{theor} \leqslant 5.2 \times 10^{-4}$ kg^2 m^{-4} s^{-1}, which is comparable to the experimental value $k_{exp} \leqslant 2.1 \times 10^{-4}$ kg^2 m^{-4} s^{-1} (see Fig. 3).

In the second case, the liquid layer thickness exceeds the critical value, $\Delta > \Delta_{cr}$ and $\Delta > h$. In this case, the gradient of oxygen concentration exists both in the channel and in the layer:

in the layer

$$\nabla c = \frac{c_0 - c_1}{\Delta}, \tag{27}$$

where $\Delta = nh$, $n > 1$, *i.e.*

$$\nabla c = \frac{c_0 - c_1}{nh}; \tag{28}$$

in the channel

$$\nabla c = \frac{c_1}{h}. \tag{29}$$

The expressions for the flux of oxygen ions have the form:

in the layer

$$J_{(\Delta)} = -D\frac{c_0 - c_1}{nh}, \tag{30}$$

in the channel

$$J_{(h)} = -D_{ef}\frac{c_1}{h}. \tag{31}$$

In the steady state

$$J_{(\Delta)} = J_{(h)}\,, \tag{32}$$

hence

$$D\frac{c_0 - c_1}{nh} = D_{ef}\frac{c_1}{h}. \tag{33}$$

Substituting (23) into (33), we obtain

$$\frac{c_0 - c_1}{n} = \frac{\delta}{l} c_1 , \tag{34}$$

whence

$$c_1 = \frac{c_0}{1 + \delta n/l}. \tag{35}$$

The equation of mass balance (14) for thick layers is written in the form

$$c^* \frac{\mathrm{d}h}{\mathrm{d}t} = D_{\mathrm{ef}} \frac{c_0}{h(1 + \delta n/l)} . \tag{36}$$

Integration of this expression gives a parabolic law of copper oxidation

$$h^2 = kt, \tag{37}$$

where

$$k = 2D_{\mathrm{ef}} \frac{c_0}{c^*} \frac{1}{1 + \delta n/l} . \tag{38}$$

Thus, the number n increases and k decreases as the layer thickens, which is in accord with experimental results.[28,29] The theory is also applicable if the rate of metal oxidation is controlled by the diffusion of cations. In this case, the picture changes symmetrically, and the liquid layer is adjacent to the metal (Fig. 12).

The suggested theory of COM is primarily valid in systems where oxidation results in the LGBS formation in the reaction products. As shown above, an LGBS is formed due to topochemical destruction or upon interaction of a liquid with grain boundaries of a solid. Therefore, the fast stage of the COM is most probable in metal – oxide systems in which formation of thermally unstable mixed or low-melting oxides is possible.

III. Super-fast stage of catastrophic oxidation of metals

1. Oxidation kinetics

In a study of the oxidation of copper under a bulk Bi_2O_3 layer thicker than 5 mm, it was found[28,29] that at the instant when Bi_2O_3 melts (point A in Fig. 13) at $m_{Bi_2O_3}/m_{Cu} \geqslant 20$, copper plates (0.5 – 1 mm thick) undergo super-fast (in 5 – 10 s) oxidation in the medium of Bi_2O_3, thus reducing the latter. If $m_{Bi_2O_3}/m_{Cu} < 20$, only the amount of copper equal to 1/20 of the Bi_2O_3 mass is oxidised super-fast, while the rest of copper is oxidised much more slowly. The $m_{Bi_2O_3}/m_{Cu}$ ratio at which super-fast oxidation of copper occurs depends on the partial oxygen pressure p_{O_2}: when p_{O_2} decreases, $m_{Bi_2O_3}/m_{Cu}$ decreases as well. The minimum value $m_{Bi_2O_3}/m_{Cu} = 3.6$ is reached at $p_{O_2} \approx 10^2$ Pa (Fig. 14).

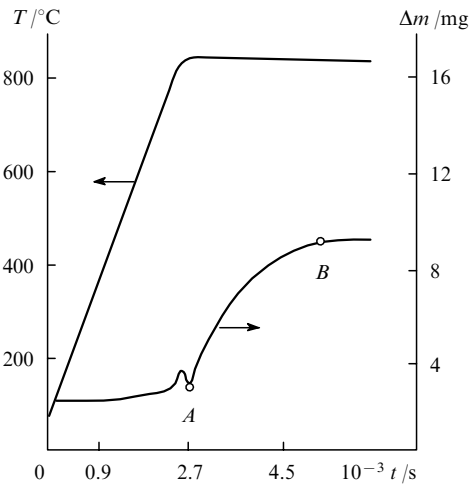


Figure 13. Kinetics of copper oxidation under a layer of Bi_2O_3 in air, $m_{Bi_2O_3} = 2.226$ g, $m_{Cu} = 0.036$ g.

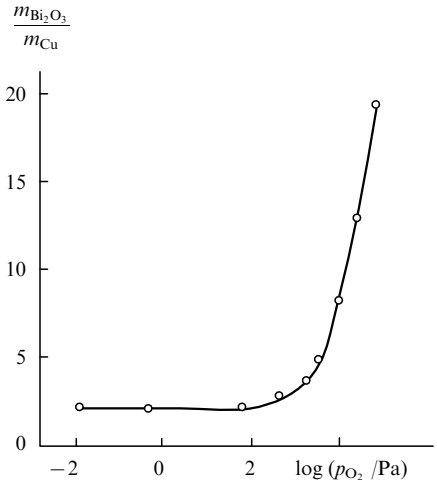


Figure 14. Dependence of the critical ratio ($m_{Bi_2O_3}/m_{Cu}$) on the oxygen partial pressure (p_{O_2}).

The literature contains controversial thermodynamic data for both the free energy of Bi_2O_3 formation and the dissociation pressure. According to some sources, copper reduces Bi_2O_3, while it does not do so according to others.[102 – 104]

2. Mechanism of the super-fast stage of catastrophic oxidation of metals

The high rate of copper oxidation under a layer of Bi_2O_3 melt at $p_{O_2} = 10^{-2} – 10^2$ Pa (see Fig. 14) can be explained as follows. The initial mass ratio $m_{Bi_2O_3}/m_{Cu} = 3.6$ corresponds to 60 mol.% of Cu_2O and 40 mol.% of Bi_2O_3 (taking into account that all of the copper is oxidised into Cu_2O and the initial amount of Bi_2O_3 decreases accordingly). According to the phase diagram of $Bi_2O_3 – Cu_2O$ (see Fig. 9), the composition of 60 mol.% of Cu_2O and 40 mol.% of Bi_2O_3 and the temperature 816 °C correspond to point C on the liquidus line. If $m_{Bi_2O_3}/m_{Cu} > 3.6$, the figurative point of the system is to the left of point C, while at $m_{Bi_2O_3}/m_{Cu} = 3.6$, these points coincide. Copper is oxidised (reducing Bi_2O_3) into Cu_2O, which in turn undergoes continuous dissolution. Hence, super-fast oxidation occurs at the metal surface (without a protective oxide layer) due to a redox reaction. Withdrawal of reaction products from the reaction zone probably occurs by convective diffusion.

At $m_{Bi_2O_3}/m_{Cu} < 3.6$, a fraction of copper which is 1/3.6 of the Bi_2O_3 mass is oxidised super-fast. After that, the figurative point of the system shifts to the right of C. Copper oxide formed on the copper surface is in the solid state and does not dissolve. Subsequent dissolution of copper occurs by the diffusion mechanism.

Super-fast oxidation of the metal occurs also at higher partial oxygen pressures, so that the $m_{Bi_2O_3}/m_{Cu}$ ratio increases (see Fig. 14). In this case, the mechanism of copper oxidation does not differ in principle from that described above and the increase in $m_{Bi_2O_3}/m_{Cu}$ at which super-fast copper oxidation occurs is due to the fact that CuO is stable at $p_{O_2} \approx 6 \times 10^3$ Pa,[102] therefore the formation of Bi_2CuO_4 is possible,[39 – 42] which is in accord with experimental results.[28,29] The decrease in the amount of copper oxidised super-fast in air in comparison with the critical mass of copper oxidised *in vacuo* is due to the formation of Bi_2CuO_4 and hence depletion in the starting Bi_2O_3. Copper undergoes super-fast oxidation and reduces bismuth oxide to the metal, which is subsequently oxidised with atmospheric oxygen (section AB in Fig. 13). Simultaneously, Cu_2O is partially oxidised to CuO. The insignificant mass decrease in the kinetic curve of copper oxida-

tion in point A is due to partial dissociation of Bi_2CuO_4 according to reaction (2).

Thus, super-fast copper oxidation is caused by continuous dissolution of the protective oxide film of Cu_2O in a Bi_2O_3 melt. Oxidation occurs on a permanently bare metal surface due to a redox reaction. The critical ratio $m_{Bi_2O_3}/m_{Cu}$ at which super-fast copper oxidation occurs is determined by the position of the figurative point on the liquidus line on the $Bi_2O_3-Cu_2O$ binary phase diagram, or on the liquidus surface in a ternary diagram if mixed oxides are formed.

IV. Conclusion

It should be noted that COM can occur both according to the electrochemical mechanism (diffusion of ions along liquid intergranular channels) and according to the flux formation mechanism (dissolution of the protective oxide layer). The realisation of the particular mechanism depends on the mass ratio of the liquid phase (m_L) and the metal (m_M) and the Gibbs free energies of formation of the solid product (ΔG_1) and the liquid phase (ΔG_2).

1. If $|\Delta G_1| > |\Delta G_2|$ and $m_L/m_M \geqslant A$, where A is the number determined by the position of the figurative point of the system on the liquidus surface corresponding to a definite composition and temperature on the phase diagram. In this case, a redox reaction is possible, while the LGBS formation is impossible; the figurative point of the system is located above the liquidus surface or coincides with it. The metal oxidation occurs at a very high rate according to the flux formation mechanism. The metal is oxidised within seconds.

2. If $|\Delta G_1| > |\Delta G_2|$ and $m_L/m_M < A$, then both the redox reaction and the LGBS formation are possible. A fraction of the metal amounting to $1/A$ of the mass of the liquid phase is oxidised according to the flux formation mechanism. The figurative point of the system is then shifted below the liquidus surface. An LGBS is formed on the metal surface. Subsequent metal oxidation occurs more slowly according to the electrochemical mechanism.

3. If $|\Delta G_1| < |\Delta G_2|$ and $m_L/m_M \geqslant A$, then both the redox reaction and the LGBS formation are impossible. Both the flux formation and electrochemical mechanisms are operative, therefore, the rate of metal oxidation is much lower than that in case 1.

4. If $|\Delta G_1| < |\Delta G_2|$ and $m_L/m_M < A$, then the LGBS formation is possible but the redox reaction is impossible. The metal fraction which amounts to $1/A$ of the mass of the liquid phase is oxidised as in the preceding case. The figurative point of the system is then shifted below the liquidus surface. An LGBS is formed on the metal surface. Subsequent oxidation follows the electrochemical mechanism.

The general picture of COM can be represented as follows. The catastrophic oxidation of metals under a thin liquid layer no thicker than $\sim$100 μm occurs by the electrochemical mechanism and is caused by the LGBS formation in the corrosion product. In this case, the contribution of super-fast oxidation according to the flux formation mechanism is insignificant, as the metal fraction that undergoes super-fast oxidation is as small as 0.5% – 3%. As the layer thickness increases, the contribution of super-fast oxidation becomes greater, which would change the character of oxidation and increase the rate of the process.

Thus, the following conclusions can be made on the basis of the data presented above.

1. The fast stage of COM is caused by the LGBS formation in the corrosion product. The oxidation rate depends on the diffusion of ions along the liquid intergranular channels.

2. The super-fast stage of COM is caused by the high rate of dissolution of the protective oxide film. The oxidation occurs by a redox reaction on a continuously bare metal surface.

References

1. C Wagner *Z. Phys. Chem.* **32** 447 (1936)
2. C Wagner *Z. Angew. Chem.* **49** 735 (1936)
3. W C Leslie, M G Fontana *Trans. Am. Soc. Metals* **41** 1213 (1949)
4. M G Fontana *Ind. Eng. Chem.* **42** 65 (1950)
5. Ya B Zel'dovich *Zh. Eksp. Teor. Fiz.* **9** 159 (1939)
6. Ya B Zel'dovich *Zh. Eksp. Teor. Fiz.* **11** 159 (1941)
7. P Kofstad *High Temperature Oxidation of Metals* (New-York: Wiley, 1966)
8. E A Gulbransen, G H Meier, in *Proceedings of the 10th Symposium on Materials Research* Vol. 561 (Washington, DC: National Bureau of Standards, 1979) p. 1639
9. E A Gulbransen, K F Andrew, F A Brassart *J. Elektrochem. Soc.* **110** 952 (1963)
10. N D Tomashov, G P Chernova *Teoriya Korrozii* (The Corrosion Theory) (Moscow: Metallurgiya, 1993)
11. V V Belousov *Corros. Sci.* (1998) (in the press)
12. A De S Brasunas, N J Grant *Trans. Am. Soc. Metals* **3W** 30 (1952); *Chem. Abstr.* **46** 326a (1952)
13. S S Brenner *J. Electrochem. Soc.* **102** 7 (1955)
14. G W Rathenau, J L Meijering *Metallurgia* **42** 167 (1950)
15. J L Meijering, G W Rathenau *Nature (London)* **165** 240 (1950)
16. K R Peters, D P Whittle, J Stringer *Corros. Sci.* **16** 791 (1976)
17. M E El-Dahshan, D P Whittle, J Stringer *Corros. Sci.* **16** 83 (1976)
18. M G Cox, B Mc Enaney, V D Scott *Philos. Mag.* **29** 595 (1974)
19. M G Cox, B Mc Enaney, V D Scott *Philos. Mag.* **26** 839 (1972)
20. J A Goebel, F S Pettit, G W Goward *Metall. Trans.* **4** 261 (1973)
21. H L Logan *Corrosion* **15** 443 (1959)
22. T T Huang PhD Thesis University of Pittsburgh, Pittsburgh, 1979
23. M E El-Dahshan, D P Whittle, J Stringer *Corros. Sci.* **16** 77 (1976)
24. S S Brenner *J. Electrochem. Soc.* **102** 16 (1955)
25. K Aning, Engen. Sci. Doct. Thesis Columbia University, New York, 1976
26. V N Konev, V V Belousov *Zashchita Metallov* **25** 138 (1989)
27. V V Belousov *Oxid. Metal.* **38** 289 (1992)
28. V V Belousov *Zashchita Metallov* **30** 599 (1994)
29. V V Belousov *Oxid. Metal.* **42** 511 (1994)
30. V V Belousov, B S Bokshtein *Zashchita Metallov* **34** 36 (1998)
31. V V Belousov *Elektrokhimiya* **31** 1343 (1995) [a]
32. V V Belousov *J. Am. Ceram. Soc.* **79** 1703 (1996)
33. V V Belousov, B S Bokschtein *Oxid. Metal.* (1998) (in the press)
34. N Birks, G H Meier *Introduction to High Temperature Oxidation of Metals* (Pittsburg: E Arnold, 1983)
35. D K Gupta, R A Rapp *J. Electrochem. Soc.* **127** 2194 (1980)
36. J A Goebel, F S Pettit *Metall. Trans.* **1** 1943 (1970)
37. D R Chang, R Nemoto, J B Wagner, Jr *Metall. Trans.* **7A** 803 (1976)
38. M R Wootton, N Birks *Corros. Sci.* **12** 829 (1972)
39. J-C Boivin, O Thomas, G Tridot *C. R. Hebd. Seances Acad. Sci., Ser. C* **276** 1105 (1973)
40. B G Kakhan, V B Lazarev, I S Shaplygin *Zh. Neorg. Khim.* **24** 1663 (1979) [b]
41. Yu F Kargin, V M Skorikov *Zh. Neorg. Khim.* **34** 2713 (1989) [b]
42. M P Kulakov, D Ya Lenchinenko *Termochim. Acta* **188** 129 (1991)
43. C Changkan, H Yongle, B M Wanklyn, J B Hodby, F R Wondre *J. Mater. Sci.* **28** 5045 (1993)
44. Y Ikeda, Y Sano, Y Bando, T Niinae, J Takada *Funtai Oyobi Funmatsu Yakin* **41** 384 (1994); *Chem. Abstr.* **121** 41 029 (1994)
45. C-F Tsang, J K Meen, D Ehhon *J. Am. Ceram. Soc.* **77** 3119 (1994)
46. C Mallika, O M Sreedharan, *J. Alloys Compd.* **216** 47 (1994)
47. B Hallstedt, D Risold, L J Gauckler *J. Am. Ceram. Soc.* **79** 353 (1996)
48. G Gattow, H Schroeder *Z. Anorg. Allg. Chem.* **318** 176 (1962)
49. H A Harvig *Bismuthesguide: Phase Relations and Electric Properties, Utrecht, 1977*
50. E M Levin, R S Roth *J. Res. Nat. Bul. Stand. A, Phys. Chem.* **68** 189 (1964)
51. H A Harvig, A G Gerards *Termochim. Acta* **28** 121 (1979)
52. M Tsubaki, K Kichiro *Mater. Res. Bull.* **19** 1613 (1984)

53. H H Moebius, P Shuk, in *17 Jahrestagung Vereinigung für Kristallorgaph Gesellschaft Geologische Wissenschaften, Leipzig, 1983* S. 12
54. L G Sillen, B Aurivillins *Z. Kristallogr.* **101** 483 (1939)
55. L G Sillen, B Sillen *Z. Phys. Chem.* **49** 27 (1941)
56. G Gattow *Z. Anorg. Allg. Chem.* **298** 64 (1959)
57. H A Harvig, A G Gerards *J. Solid. State. Chem.,* **26** 265 (1978)
58. L G Sillen *Ark. Kemi. Miner. Geolog.,* **12A** 1 (1937)
59. V V Belousov, V N Konev, A K Roslik *Sverkhprovodimost: Fiz., Khim., Tekhn.* **3** 1895 (1990)
60. W W Mullins *J. Appl. Phys.* **28** 333 (1957)
61. W W Mullins *J. Appl. Phys.* **30** 77 (1959)
62. H J Vogel, L Ratke *Acta Metall. Mater.* **39** 641 (1991)
63. L G Pertsov, L A Pogosyan, B D Summ, Yu V Goryunov *Kolloidn. Zh.* **36** 699 (1974) [c]
64. V V Belousov *J. Am. Ceram. Soc.* (1998) (in the press)
65. L A Pogosyan, Yu V Goryunov, V Yu Traskin *Vestn. Mosk. Univ., Ser. 2, Khim.* **5** 589 (1974) [d]
66. K Nord-Varhaug *J. Am. Ceram. Soc.* **79** 1147 (1996)
67. S Ramamuthy, M P Mallamaci, C B Carter *Scr. Mater.* **34** 1779 (1996)
68. N Eustathopoulos, L Condurier, J Loud, P Desre *J. Cryst. Growth.* **33** (1) 105 (1976)
69. A Passerone, R Sangiorgi, N Eustathopoulos *Scr. Metall.* **14** 1089 (1980)
70. A Passerone, R Sangiorgi, N Eustathopoulos *Scr. Metall.* **16** 547 (1982)
71. A Passerone, R Sangiorgi *Acta Metall.* **33** 77 (1985)
72. W W Mullins *Metall. Mater. Trans. A, Phys. Metall. Mater. Sci.* **26** 1917 (1995)
73. A Passerone, N Eustathopoulos *Acta Metall.* **30** 1349 (1982)
74. F N Rhines, B R Patterson *Metall. Mater. Trans. A, Phys. Metall. Mater Sci.* **13** 985 (1982)
75. B S Bokstein, L M Klinger, I V Apikhtina *Mater Sci. Eng. A, Sctruct. Mater., Prop. Mikrostruct. Proc.* **203** 373 (1995)
76. W M Robertson *Trans. Metall. Soc.* **233** 1232 (1965)
77. W M Robertson *J. Appl. Phys.* **42** 463 (1971)
78. B S Allen *Trans. Metall. Soc. AIME* **245** 1621 (1969)
79. V V Belousov, B S Bokshtein *Poverkhnost* (1998) (in the press)
80. R L Kluch *Trans. Am. Nucl. Soc.* **15** 746 (1972)
81. V E Fradkov *Scr. Metall. Mater.* **30** 1599 (1994)
82. P L Flaitz and J Pask *J. Am. Ceram. Soc.* **70** 449 (1987)
83. T M Shaw *J. Am. Ceram. Soc.* **74** 2495 (1991)
84. E L Rabkin, V N Semenov, L S Shwindlerman, B B Straumal *Acta Metall.* **39** 627 (1991)
85. D R Clarke, M L Gee, in *Materials Interfaces. Atomic-Level Structure and Properties* (Eds D Wolf, S Yip) (London: Chapman and Hall, 1992) p. 255
86. E A Prodan *Neorganicheskaya Topokhimiya* (Inorganic Topochemistry) (Minsk: Nauka i Tekhnika, 1986)
87. E A Prodan *J. Thermal Anal.* **29** 941 (1984)
88. V N Chebotin *Khimicheskaya Diffuziya v Tverdykh Telakh* (Chemical Diffusion in Solids) (Moscow: Nauka, 1989)
89. V N Chebotin, M V Perfil'ev *Elektrokhimiya Tverdykh Elektrolitov* (Electrochemistry of Solid Electrolytes) (Moscow: Khimiya, 1978)
90. S Chandra *Superionic Solids* (Amsterdam: North Holland, 1981)
91. J W Perram (Ed.) *Physics of Superionic Conduct and Electrode Materials* (New York: Plenum, 1983)
92. A L Laskar, S Handra (Eds) *Superionic Solids and Solid Electrolytes — Recent Trends* (New York: Academic Press, 1989)
93. J C Maxwell, in *A Treatise on Electricity and Magnetism* Vol. 1 (Oxford: Clarendon Press, 1881) p. 403
94. V I Odelevskii *Zh. Tekh. Fiz.* **21** 661 (1951)
95. B N Shklovskii, A L Efros *Elektricheskie Svoistva Legirovannykh Poluprovodnikov* (Electrical Properties of Alloyed Semiconductors) (Moscow: Nauka, 1979)
96. D J Bergman, in *Electrical Transport and Optical Properties of Inhomogeneous Media* (New York: American Physics Institute, 1978) p. 46
97. S Kirkpatrick *Rev. Mod. Phys.* **45** 574 (1973)
98. I L Tallon, W H Robinson, S Smedley *J. Phys. C* **10** L579 (1977)
99. M Yan, R Cannon, H Bowen, R Coble *J. Am. Ceram. Soc.* **60** 120 (1977)
100. C C Liang *J. Electrochem. Soc.* **120** 1289 (1973)
101. E W Hart *Acta Metall.* **5** 597 (1957)
102. O Kubashevskii, S B Allcock *Metallurgicheskaya Termokhimiya* (Metallurgical Thermochemistry) (Translated into Russian; (Moscow: Metallurgiya, 1982)
103. P Schuk, S Jakobs, H Moebius *Haupt. Chem. Ges. DDR* 100 (1980)
104. N A Vasil'eva, A F Maiorova *Dokl. Akad. Nauk SSSR* **280** 385 (1985) [e]

[a] — *Electrochemistry (Engl. Transl.)*
[b] — *Russ. J. Inorg. Chem. (Engl. Transl.)*
[c] — *Colloid J. (Engl. Transl.)*
[d] — *Moscow Univ. Bull. (Engl. Transl.)*
[e] — *Dokl. Chem. Technol., Dokl. Chem. (Engl. Transl.)*